

An off-lattice Wang-Landau study of the coil-globule and melting transitions of a flexible homopolymer

Drew F. Parsons and David R. M. Williams

Citation: *J. Chem. Phys.* **124**, 221103 (2006); doi: 10.1063/1.2209684

View online: <http://dx.doi.org/10.1063/1.2209684>

View Table of Contents: <http://jcp.aip.org/resource/1/JCPSA6/v124/i22>

Published by the [AIP Publishing LLC](http://www.aip.org).

Additional information on *J. Chem. Phys.*

Journal Homepage: <http://jcp.aip.org/>

Journal Information: http://jcp.aip.org/about/about_the_journal

Top downloads: http://jcp.aip.org/features/most_downloaded

Information for Authors: <http://jcp.aip.org/authors>

ADVERTISEMENT



Explore the **Most Cited**
Collection in Applied Physics

AIP
Publishing

An off-lattice Wang-Landau study of the coil-globule and melting transitions of a flexible homopolymer

Drew F. Parsons^{a)} and David R. M. Williams

Research School of Physical Sciences and Engineering, Australian National University, Canberra, ACT 0200, Australia

(Received 2 March 2006; accepted 10 May 2006; published online 13 June 2006)

The Wang-Landau Monte Carlo approach is applied to the coil-globule and melting transitions of off-lattice flexible homopolymers. The solid-liquid melting point and coil-globule transition temperatures are identified by their respective peaks in the heat capacity as a function of temperature. The melting and theta points are well separated, indicating that the coil-globule transition occurs separately from melting even in the thermodynamic limit. We also observe a feature in the heat capacity between the coil-globule and melting transitions which we attribute to a transformation from a low-density liquid globule to a high-density liquid globule. © 2006 American Institute of Physics. [DOI: 10.1063/1.2209684]

The Wang-Landau Monte Carlo technique¹ has recently been promoted as a tool for calculating phase transitions.^{2,3} Since the density of states $g(E)$ is independent of temperature, it encapsulates a system's behavior, such as internal energy $U(T)$, at all temperatures in the one calculation. The heat capacity may be readily computed as $C_V=dU/dT$, and phase transitions such as the solid-liquid melting point may be identified by peaks in $C_V(T)$.

A calculation of this nature studying the coil-globule transition of flexible homopolymers was recently performed by Rampf *et al.*,⁴ who used a lattice model with a square-well interaction energy between monomers. They measured the solid-liquid and coil-globule transition temperatures and concluded that in the thermodynamic limit, the two transition temperatures coincide, with the swollen coil bypassing the liquid globule and collapsing directly to the solid globule.

Independently we have been pursuing a similar study. We have implemented⁵ the Wang-Landau algorithm using an off-lattice model incorporating a finitely extensible nonlinear elastic (FENE) bond potential between neighboring bonded monomers, $E_{\text{bond}}=-KR^2 \ln(1-((l-l_0)/(l_{\text{max}}-l_0))^2)$, and a Lennard-Jones two-body potential between all monomers. The average bond length was $l_0=0.7$, bound in the range $l \in (0.4, 1.0)$ with spring constant $K=20$. The Lennard-Jones parameters were aligned so that the Lennard-Jones energy minimum coincided with the FENE bond length, i.e., $\sigma=l_0/2^{1/6}$ and $\epsilon=1$. The microcanonical ensemble average of a range of values including the radius of gyration and the core density (defined as the number of monomers in a sphere of radius 2.5σ around the monomer closest to the polymer's centre of mass) were calculated for each energy bin E and converted to a canonical ensemble average, e.g., $\langle R_g^2(T) \rangle$, using the density of states. Calculations were performed for N between 50 and 300. The density of states $g(E)$ was determined within the range $E \in [-4N, 0)$, which allows temperature behavior to be deter-

mined in the range $T \in (0.5, 3)$, wide enough to cover the transitions described here.

Sample densities of states for $N=100, 200$, and 300 are given in Fig. 1, shifted to a common value of 2000 at $E=0$. Heat capacity curves $C_V(T)$ generated from the density of states for $N=100, 200$, and 300 are shown in Fig. 2. Repeated calculations at each N are given, each based on a different starting configuration of the polymer. Constraints in the computer time available mean there is some variation between the curves repeated for a given N , resulting in a deviation of about ± 0.05 in the temperature positions of the peaks representing the melting and coil-globule transitions. We identify three sites of interest, marked as regions I, II, and III around temperatures $T=0.8, 1.2$, and 2 , respectively. The peaks at regions I and III become sharper as N increases, characteristic of a well-defined transition. The region II feature suggests a reorganization is occurring inside the liquid globule.

The radius of gyration for $N=100, 200$, and 300 is given in Fig. 3, showing an increasingly steep slope in the transition region as N increases, again characteristic of a well-

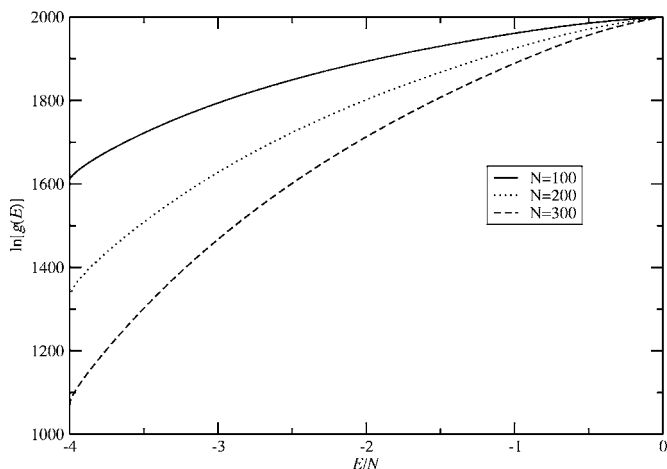


FIG. 1. Density of states (log representation) for $N=100, 200$, and 300 .

^{a)}Electronic address: Drew.Parsons@anu.edu.au

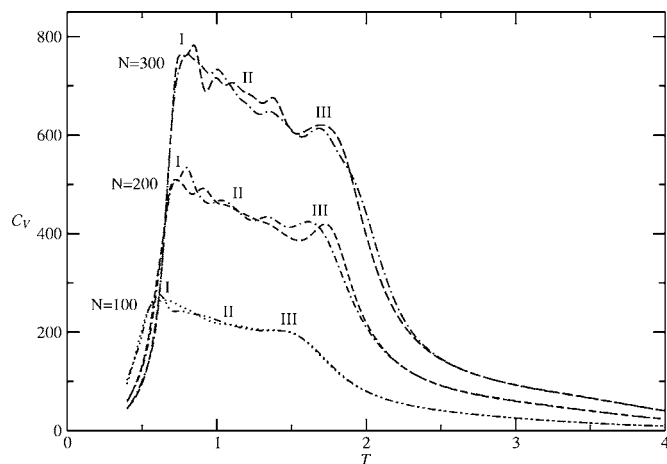


FIG. 2. Heat capacity $C_V=dU/dT$ (repeated calculations shown for $N=100, 200,$ and 300).

defined transition. The point of steepest slope occurs around $T=2$, the same temperature as the region III (highest temperature) C_V peak, hence we identify this peak with the coil-globule transition. Core density is plotted against temperature in Fig. 4, also exhibiting a number of stationary points in the derivative where the density of the globule is suddenly increased, matching the features in the heat capacity.

We identify the lowest temperature transition point at peak I as the solid-liquid melting point since it is the largest peak in the heat capacity curve. We expect that the size of the peak would be larger for a solid-liquid transition than for a liquid-liquid or solid-solid transition. It follows that the middle region II corresponds to compactification inside the liquid-like globule. In the absence of such a liquid-liquid reorganization we would expect a single trough to lie between the solid-liquid and coil-globule transition peaks, rather than the structure seen at region II in Fig. 2. Moreover, we read from Fig. 4 that after coil-globule collapse, the core density in the newly formed liquid globule at region III is about 30 monomers per core sphere, barely half of its final value around 55 monomers per core sphere at region I where solidification occurs. Substantial compactification therefore occurs within the liquid globule in region II, between regions

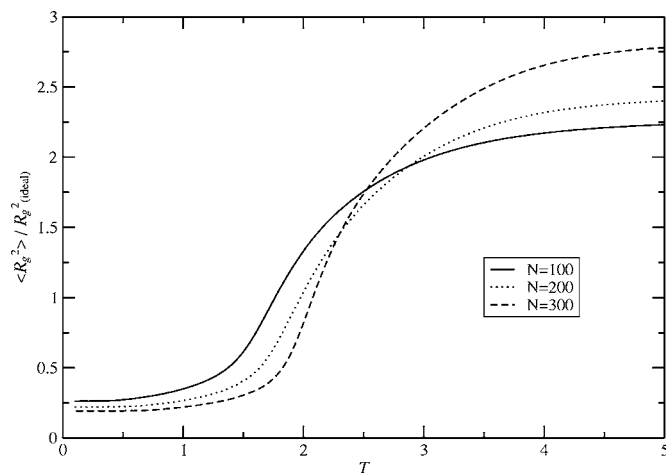


FIG. 3. Radius of gyration squared as a function of temperature, for $N=100, 200,$ and 300 , scaled against the radius of gyration squared for an ideal coil, $R_{g(\text{ideal})}^2=N(l_0)^2/6$.

I and III, resulting in the region II features seen in the heat capacity. Buldyrev *et al.*⁶ describe a phase transition between high-density liquid and low-density liquid in a model contain two characteristic repulsive distances. This is consistent with our interpretation of region II as a region of compactification between high-density and low-density liquid globule, with the two length scales arising from FENE repulsion between bonded monomers and from the Lennard-Jones interactions. The liquid or solid nature of the regions may be confirmed by molecular dynamics calculations measuring the mean free displacement of the monomers in each region.

The melting point and coil-globule transitions have been well characterized in the literature.⁷⁻¹⁰ The intermediate liquid-liquid reorganization has not been reported previously, although a subtle hint of it for small polymers ($N=30, 64$) may be seen as a slight shoulder in the heat capacity in Fig. 1 of both Refs. 9 and 10, coincidentally at $T \approx 0.5$ reduced units in both cases. Being small in these previous studies, this shoulder was left unremarked upon by the respective authors. The feature is similarly small in our calculations at $N=100$, only becoming noticeable at larger N . The curves in Fig. 2 suggest that the compactification corresponding to the

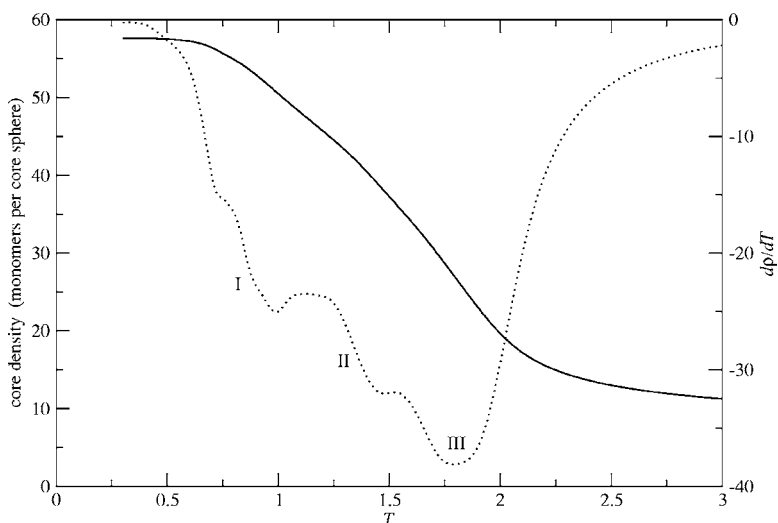


FIG. 4. Core density and its derivative with respect to temperature (shown for $N=300$). Core density is defined as the number of monomers in a sphere of radius 2.5σ from the monomer closest to the center-of-mass. The solid line represents the density, the dotted line is its derivative.

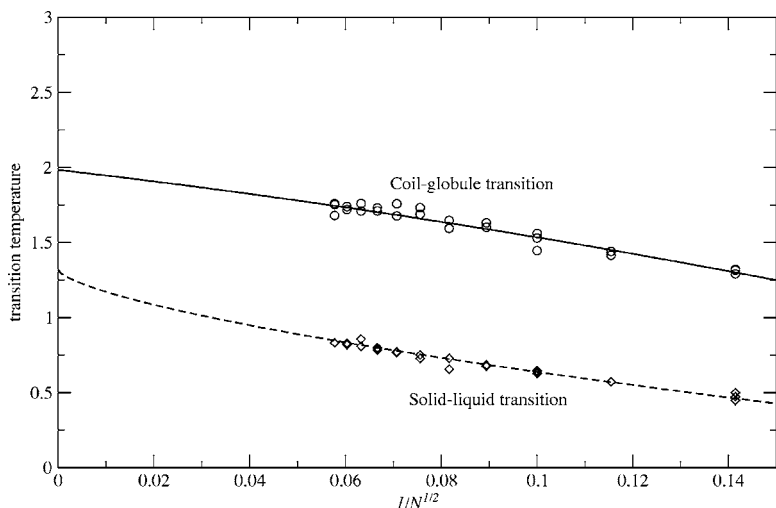


FIG. 5. Scaling of transition temperatures. The top curve represents the coil-globule transition, determined by peak III in heat capacity for each N , with $\Theta=1.98$. The lower curve is interpreted as the solid-liquid melting point (peak I in heat capacity) with $T_M=1.317$. Data are plotted against $1/\sqrt{N}$ to show extrapolated behavior of the solid-liquid and coil-globule transitions at large N .

region II feature may possibly resolve into two steps. This could correspond to the formation of layers within the high-density liquid globule¹¹ or to a preferential globule size constrained by monomer connectivity in the polymer chain.

We calculated the theta point Θ derived from fitting the peak III transition points for each N . These were calculated from a density of states curve smoothed to an order 10 polynomial in order to minimize the effect of noise. The energy range $E \in [-4N, 0)$ was selected to facilitate this smoothing, since at higher E the density of states $\ln[g(E)]$ becomes more flat, unsuitable for a polynomial fit. The process smoothed region II into a single peak but made the region I and III peaks more easily determined, while still within the deviation of about $T \pm 0.05$ seen between different curves calculated at the same N . The points $T_\Theta(N)$ for each N were fitted to the functional form⁴

$$T_\Theta(N) = \Theta - \frac{A_1}{\sqrt{N}} + \frac{A_2}{N}. \quad (1)$$

The fit, shown in Fig. 5, gave us a theta point of $\Theta=1.98 \pm 0.13$, with $A_1=3.67$ and $A_2=-8.24$. Formula (1) contains no log correction,¹² resulting in an overestimation of the theta point in Ref. 4 compared to that calculated in Ref. 13. Given the slight downward curvature in the transition III data at large N in Fig. 5, we might ask if the log correction could significantly reduce the estimate for the theta temperature, affecting the comparison given below with the melting point. However in our case the log-corrected formula¹²

$$T_\Theta(N) = \Theta - \frac{A}{\sqrt{N}(\ln N)^{7/11}}, \quad (2)$$

generates nearly the same theta point from our peak III data, $\Theta=1.953 \pm 0.026$ (with $A=11.04$), only slightly lower than the estimate from Eq. (1) and still within its error bounds.

The melting point T_M was calculated by fitting the peak I temperatures T_{tr} for each N (see Fig. 5) to

$$T_{tr} = T_M - \frac{B}{\sqrt[3]{N}}, \quad (3)$$

yielding $T_M=1.317 \pm 0.033$, with $B=3.15$. This melting point is significantly lower than the coil-globule transition theta point, with ratio $\Theta/T_M=1.50$. The separation of temperatures is sustained even if the extreme values of the estimates after adding error bars are considered. This contrasts strongly with the results of Rampf *et al.* where the two transition temperatures coincided. Our model provides an example of a system where, in different conditions (off-lattice, FENE, and Lennard-Jones interactions), the coil-globule transition is maintained distinct from the solid-liquid transition. The difference is probably due largely to our use of an off-lattice model, although the longer range interactions afforded by the Lennard-Jones potential, compared to the short square well potential used by Rampf *et al.* may also contribute to the difference.

In conclusion, we have characterized the structure in the heat capacity of a single flexible homopolymer, identifying a solid-liquid and coil-globule transition as well as a compaction transformation inside the liquid globule. Our model provides an example where the theta point is significantly higher than the solid-liquid melting point.

The authors would like to thank Wolfgang Paul for useful discussions. This work was supported by an Australian ARC Discovery Grant.

¹D. P. Landau, S.-H. Tsai, and M. Exler, *Am. J. Phys.* **72**, 1294 (2004).

²N. Wilding and D. P. Landau, *Monte Carlo Methods for Bridging the Timescale Gap*, in *Lecture Notes in Physics* (Springer-Verlag GmbH, Berlin-Heidelberg, 2002), Vol. 605, Chap. 8, pp. 231–266.

³M. S. Shell, P. G. Debenedetti, and A. Z. Panagiotopoulos, *Phys. Rev. E* **66**, 056703 (2002).

⁴F. Rampf, W. Paul, and K. Binder, *Europhys. Lett.* **70**, 628 (2005).

⁵D. Parsons and D. R. M. Williams (in preparation).

⁶S. V. Buldyrev, G. Franzese, N. Giovambattista, G. Malescio, M. R. Sadr-Lahijany, A. Scala, A. Skibinsky, and H. E. Stanley, *Physica A* **304**, 23 (2002).

⁷J. M. Polson and N. E. Moore, J. Chem. Phys. **122**, 024905 (2005).

⁸J. M. P. van den Oever, F. A. M. Leermakers, G. J. Fleer, V. A. Ivanov, N. P. Shusharina, A. R. Khokhlov, and P. G. Khalatur, Phys. Rev. E **65**, 041708 (2002).

⁹H. Liang and H. Chen, J. Chem. Phys. **113**, 4469 (2000).

¹⁰Y. Zhou, C. K. Hall, and M. Karplus, Phys. Rev. Lett. **77**, 2822 (1996).

¹¹E. Ruckenstein and Y. S. Djikaev, Adv. Colloid Interface Sci. **118**, 51 (2005).

¹²P. Grassberger and R. Hegger, J. Chem. Phys. **102**, 6881 (1995).

¹³P. Grassberger, Phys. Rev. E **56**, 3682 (1997).